acta physica slovaca vol. 51 No. 6, 307 – 337 **December 2001**

MULTIDIMENSIONAL NUCLEAR DATA COMPRESSION USING FAST ADAPTIVE WALSH-HAAR TRANSFORM

M. Morháč, V. Matoušek[1]
Institute of Physics, Slovak Academy of Sciences, Dúbravská cesta 9, SK-842 28 Bratislava, Slovakia

Received 9 May 2001, in final form 9 November 2001, accepted 12 November 2001

The paper defines the calculation algorithms of multidimensional adaptive fast Walsh-Haar transforms (WHT) aimed for block data compression with specific needs for multidimensional nuclear (or similar) data. Example data compressed via the adaptive WHT, classical WHT and Cosine transforms are presented. The compression efficiency of adaptive transforms is evidently better than that of other classical transforms. The influence of the transform degree of WHT on the compression efficiency is also studied in the paper.

PACS: 29.85.+c, 02.60.-x, 07.05.Kf, 02.30.Qy

1 Introduction

The classical techniques developed to analyse 2-fold $\gamma - \gamma$ coincidence data (two-dimensional histograms) cannot be extended to higher-fold data. For example if we assume that the content of each channel is represented by one byte, the storage of a five-dimensional histogram with 1024 channels per axis would require a total of 1024 terrabytes of memory.

The classical method to reduce the memory requirements, which is frequently employed, is to store data in the form of lists of events. In list mode, the memory needed to save complete data from an experiment is proportional to the total number of events and also number of bytes used to store each individual event. However to have a sufficient statistic in multidimensional space, the amount of data to be collected in one experiment can be well over $10^9 \div 10^{10}$ events. For such a large amount of data there is usually not enough storage capacity available. The method proposed in the paper considerably decreases the memory needed to store multidimensional histograms. It is based on fast orthogonal adaptive transform.

Suitable distribution of signal energy in the transform domain, possibly its concentration in a small number of elements in a predetermined region of a new field, is the basic premise of successful application of an orthogonal transform in multidimensional block data compression. The transform, which concentrates the energy of signals of a given class (classes) in efficient way plays the key role to assure a good block data compression.

[1]E-mail address: matousek@savba.sk

When applying orthogonal transforms in data compression the complexity of computational algorithm is also very important factor. Because the Walsh transform (WT) [1] is binary valued its implementation is very simple. Algorithms of WT require only additions (subtractions). The number of additions to transform a vector with size N using the fast WT is proportional to $N \log_2 N$. The fastest and simplest among all orthogonal transforms is the Haar transform (HT) [1]. In essence it is also binary valued and thus requires only additions (subtractions). The number of additions in this case is equal to $2(N-1)$.

The suitability of employing a transform in the compression depends on the type of the compressed signal. For signals with dominant sharp narrow objects (peaks) the Haar transform is more efficient. On the other hand for signals containing wide objects better quality of compression can be achieved by employing the WT. The HT is locally sensitive whereas the WT is globally sensitive.

Between the Haar and Walsh transforms one can define k Walsh-Haar transforms (WHT), where $k = \log_2 N$ and N is the transform length. Then WHT of ($\log_2 N - 1$)-st degree is identical with the WT and WHT of 0-th degree is identical with the HT. By increasing the degree of WHT the sensitivity width and thus the number of needed operations (additions and subtractions) also increases. One of the aims of the paper is the determination of optimal degree of WHT according to the class of compressed signals. The optimal degree depends on the size of objects which we want to preserve in the compressed signal.

However this is only one degree of freedom by which we can influence the efficiency and the computational complexity of the compression. The base functions of binary valued transforms do not reflect in any way the shape of the transformed signal. Classical WHT are well suited to compress signals with dominant rectangular components. In order to obtain the energy distribution in the transform domain more amenable to retaining the shape of the signal, one can modify base functions of a transform in such a way as to achieve maximum compression at the minimum signal distortion. In the paper the fast adaptive WHT ($AWHT$) is defined. The multiplication coefficients of signal flow graph of the fast transform algorithm are modified on the basis of maximum compression according to a given data class which is represented for each dimension by one vector. Hereafter this vector will be called reference vector.

The aim of the paper is to define adaptive Walsh-Haar transform ($AWHT$). The multiplication coefficients of signal flow graph of the fast algorithm to calculate $AWHT$ are modified according to maximum compression criterion with respect to a data class.

2 Fast algorithm to calculate Walsh-Haar transform of k-th degree

Classical WT and HT are very well known [1] , [2], [3]. As mentioned above these are the marginal cases of the Walsh-Haar transform set for the degrees $k = 0$ and $k = log_2 N - 1$. In [4] the WHT matrix is defined through the use of Hadamard and Haar matrices

$$\mathbf{WHT}_{2^n}^k = \mathbf{HAD}_{2^k} \otimes \mathbf{HAAR}_{2^{n-k}}, \tag{1}$$

where k denotes the degree of the transform, $N = 2^n$ is the length of the transform, $\otimes$ denotes Kronecker product of matrices. The right lower index represents the size of matrix and the right upper index represents the degree of transform. The Hadamard transform matrix is defined by

the recursive relation

$$\mathbf{HAD}_{2^k} = \mathbf{HAD}_{2^{k/2}} \otimes \mathbf{HAD}_2$$

where

$$\mathbf{HAD}_2 = \begin{bmatrix} 1 & 1 \\ 1 & -1 \end{bmatrix}.$$

The Haar matrix can be obtained from Haar functions [1], [2] or from recursive relations given in [4], [5].

The fast Cooley-Tukey's algorithm [1] to calculate the WT (or WHT^2) of the vector $\mathbf{x}$ for $N = 8$ is shown in Fig. 1.

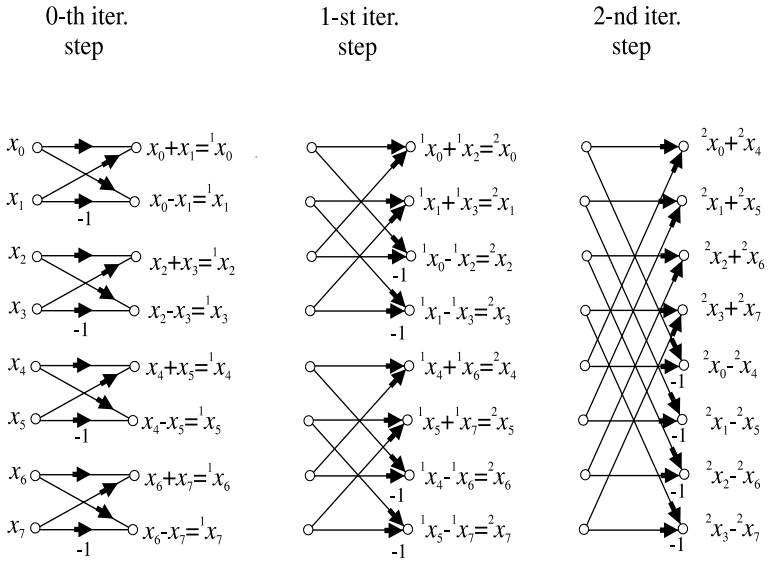

Fig. 1. Signal flow graph of the fast WHT^2 (WT) for $N = 8$

If we stop the calculation of odd indexed transform coefficients after the 1-st iteration step we get the WHT of the first degree (Fig. 2)

And finally let us stop the calculation of transform coefficients with positions $i \in \{0, \ldots, 7\}$ satisfying the condition $i \mod 2 \neq 0$ after the 0-th iteration step and coefficients satisfying the condition $i \mod 4 \neq 0$ after the 1-st iteration step. Then we obtain WHT^0 which is identical with the HT (Fig. 3).

Then in general in the Cooley-Tukey's signal flow graph of the fast WHT^k we stop the

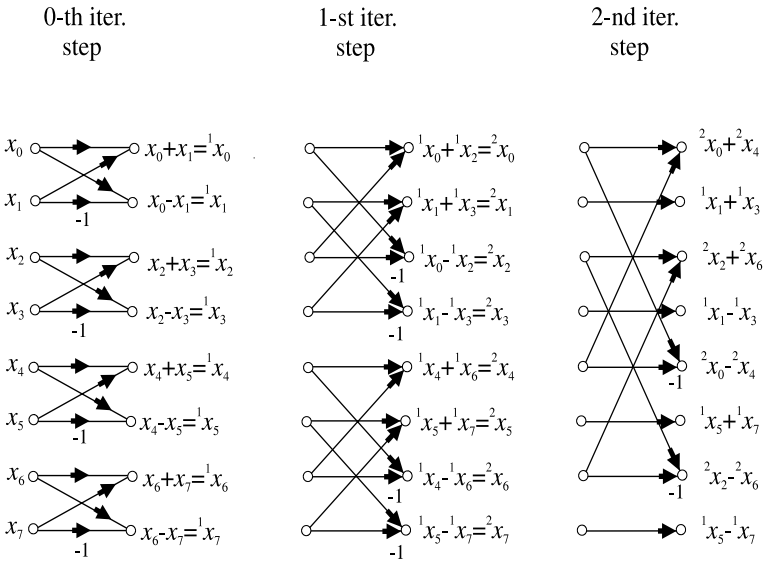

Fig. 2. Signal flow graph of the fast WHT^1 for $N = 8$

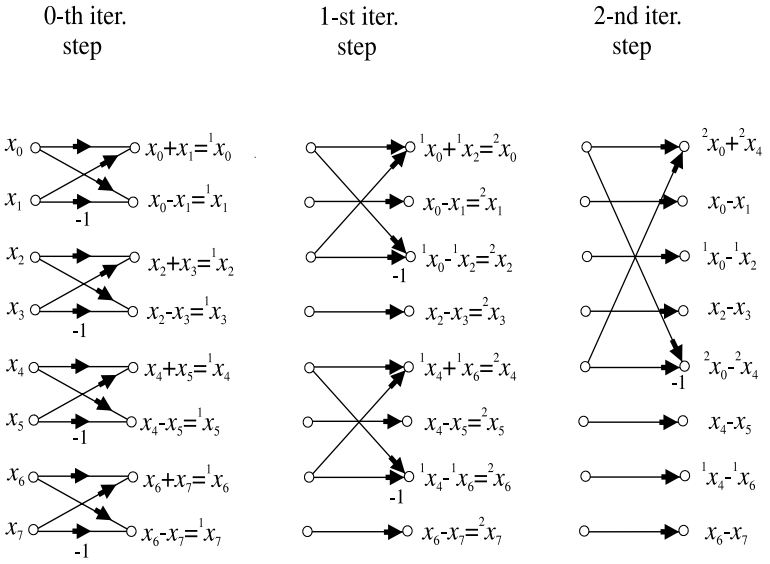

Fig. 3. Signal flow graph of the fast WHT^0 (HT) for $N = 8$

calculation after

$$\begin{aligned}
&k\text{-th iteration step for positions where} && i \mod 2 \neq 0\\
&k+1\text{-st iteration step for positions where} && i \mod 4 \neq 0\\
&\vdots\\
&k+m\text{-th iteration step for positions where} && i \mod 2^{m+1} \neq 0\\
&\vdots\\
&n-2\text{-nd iteration step for positions where} && i \mod 2^{n-1} \neq 0.
\end{aligned} \tag{2}$$

We have not considered the order of coefficients in the output transformed vector nor the scaling factors of Haar functions [1], [2]. However for the moment this is irrelevant.

From above proposed algorithm and from Figs. 1, 2, 3 one can observe that in each of iteration steps 0 to k-1 we carry out 8 additions (subtractions)(in general case N additions). Then in the k-th iteration step we carry out 8 additions, in $(k+1)$-st iteration step 4 additions etc. In general case the number of additions is

$$\begin{aligned}
N_A &= k \cdot N + N + N/2 + N/2^2 + \ldots + N/2^{\log_2 N - k - 1}\\
&= k \cdot N + N\left(1 + 1/2 + 1/2^2 + \ldots + \frac{1}{2^{\log_2 N - k - 1}}\right).
\end{aligned} \tag{3}$$

The expression in parenthesis represents sum of geometric series and can be further simplified as

$$\begin{aligned}
N_A &= k \cdot N + 2N\left(1 - \frac{1}{2^{\log_2 N - k}}\right)\\
&= k \cdot N + 2\left(N - 2^k\right).
\end{aligned} \tag{4}$$

3 Adaptive Walsh-Haar transform of k-th degree

Let the reference vector $\mathbf{x}$ represent (in a way described in the next section) the data to be transformed. Without loss of generality we shall start with the example of $AWHT^0$ and $AWHT^1$ for $N = 4$. Fig. 4 shows the signal flow graph for $AWHT^1$ where multiplication coefficients, as opposed to classical WHT, are not equal to 1. The aim of the construction of $AWHT$ is to find the coefficients a_i, b_i, c_i, d_i.

From Fig. 4 for the vector $\mathbf{y}$ one can write

$$\begin{bmatrix} y_0\\ y_1\\ y_2\\ y_3 \end{bmatrix} = \begin{bmatrix} a_2a_0 & a_2c_0 & c_2a_1 & c_2c_1\\ a_3b_0 & -a_3d_0 & c_3b_1 & -c_3d_1\\ b_2a_0 & b_2c_0 & -d_2a_1 & -d_2c_1\\ b_3b_0 & -b_3d_0 & -d_3b_1 & d_3d_1 \end{bmatrix} \begin{bmatrix} x_0\\ x_1\\ x_2\\ x_3 \end{bmatrix}, \tag{5}$$

or

$$\mathbf{y} = \mathbf{WHT}^1 \cdot \mathbf{x}. \tag{6}$$

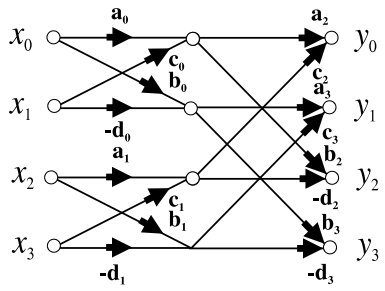

Fig. 4. Signal flow graph of the fast $AWHT^1$ for $N = 4$

The transform matrix of $AWHT^1$ should be orthonormal. Then the multiplication of $AWHT^1$ by its transpose must give the unit matrix

$$\begin{bmatrix} a_2a_0 & a_2c_0 & c_2a_1 & c_2c_1 \\ a_3b_0 & -a_3d_0 & c_3b_1 & -c_3d_1 \\ b_2a_0 & b_2c_0 & -d_2a_1 & -d_2c_1 \\ b_3b_0 & -b_3d_0 & -d_3b_1 & d_3d_1 \end{bmatrix} \begin{bmatrix} a_2a_0 & a_3b_0 & b_2a_0 & b_3b_0 \\ a_2c_0 & -a_3d_0 & b_2c_0 & -b_3d_0 \\ c_2a_1 & c_3b_1 & -d_2a_1 & -d_3b_1 \\ a_2c_1 & -c_3d_1 & -d_2c_1 & d_3d_1 \end{bmatrix} = \mathbf{E}. \tag{7}$$

This product is a symmetrical matrix. Let us take its right upper part including its main diagonal. Then one gets the following 10[†] conditions

$$\begin{aligned} \left(a_0^2 + c_0^2\right) a_2^2 + \left(a_1^2 + c_1^2\right) c_2^2 &= 1, \\ \left(a_0b_0 - c_0d_0\right) a_2a_3 + \left(a_1b_1 - c_1d_1\right) c_2c_3 &= 0, \\ \left(a_0^2 + c_0^2\right) a_2b_2 - \left(a_1^2 + c_1^2\right) c_2d_2 &= 0, \\ \left(a_0b_0 - c_0d_0\right) a_3b_3 - \left(a_1b_1 - c_1d_1\right) c_2d_3 &= 0, \\ \left(b_0^2 + d_0^2\right) a_3^2 + \left(b_1^2 + d_1^2\right) c_3^2 &= 1, \\ \left(a_0b_0 - c_0d_0\right) a_3b_2 - \left(a_1b_1 - c_1d_1\right) c_3d_2 &= 0, \\ \left(b_0^2 + d_0^2\right) a_3b_3 - \left(b_1^2 + d_1^2\right) c_3d_3 &= 0, \\ \left(a_0^2 + c_0^2\right) b_2^2 + \left(a_1^2 + c_1^2\right) d_2^2 &= 1, \\ \left(a_0b_0 - c_0d_0\right) b_2b_3 + \left(a_1b_1 - c_1d_1\right) d_2d_3 &= 0, \\ \left(b_0^2 + d_0^2\right) b_3^2 + \left(b_1^2 + d_1^2\right) d_3^2 &= 1. \end{aligned} \tag{8}$$

The conditions (8)are satisfied if

$$a_ib_i - c_id_i = 0, \tag{9}$$

$$a_i^2 + c_i^2 = 1, \tag{10}$$

$$b_i^2 + d_i^2 = 1, \tag{11}$$

[†] $((N^2 + N)/2 = 10)$

where $i = 0, \ldots, 3$. Substituting from (9)

$$a_i = \frac{c_i d_i}{b_i}, \tag{12}$$

into (10) and (11) one obtains

$$b_i^2 = c_i^2,$$

and thus

$$b_i = \pm c_i. \tag{13}$$

Substituting back from (13) into (12) we have

$$a_i = \pm d_i. \tag{14}$$

Then (9), (10), (11), (13), (14) are necessary and sufficient conditions assuring the orthonormality of $AWHT^1$.

Fig. 5 shows the adaptive WHT of the degree 0 for $N = 4$.

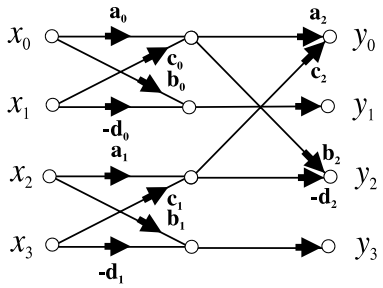

Fig. 5. Signal flow graph of the fast $AWHT^0$ for $N = 4$

Analogously to (7), (8) the conditions of orthonormality of the matrix of $AWHT^0$ are

$$\begin{aligned}
\left(a_0^2 + c_0^2\right) a_2^2 + \left(a_1^2 + c_1^2\right) c_2^2 &= 1,\\
\left(a_0 b_0 - c_0 d_0\right) a_2 &= 0,\\
\left(a_0^2 + b_0^2\right) a_2 b_2 - \left(a_1^2 + c_1^2\right) c_2 d_2 &= 0,\\
-\left(a_1 b_1 - c_1 d_1\right) c_2 &= 0,\\
b_0^2 + d_0^2 &= 0,\\
\left(a_0 b_0 - c_0 d_0\right) b_2 &= 0,\\
\left(a_0^2 + c_0^2\right) b_2^2 + \left(a_1^2 + c_1^2\right) d_2^2 &= 1,\\
\left(a_1 b_1 - c_1 d_1\right) d_2 &= 0,\\
b_1^2 + d_1^2 &= 1.
\end{aligned} \tag{15}$$

Comparing to (8) one can observe that in this case

$$a_3 = d_3 = 1; \qquad b_3 = c_3 = 0 \tag{16}$$

and therefore for $i = 3$ the conditions (9), (10), (11) are satisfied. Further it is obvious that if the conditions (9), (10), (11), (13), (14) are satisfied for $i = 0, 1, 2$ then the conditions (15) are also satisfied. Apparently for greater N and all transform degrees $k = 0, 1, \ldots, \log_2 N - 1$, if the conditions (9), (10), (11) applied to multiplication coefficients in basic computational elements - butterflies are satisfied, then the condition of orthonormality of the whole matrix of $AWHT^k$ is also satisfied. The butterflies that do not enter the calculation satisfy implicitly the conditions of orthonormality ($a_j = d_j = 1$, $b_j = c_j = 0$).

For each transform element, butterfly, we shall require that the input energy is equal to the output energy (Parseval's theorem)

$$x_0^2 + x_1^2 = y_0^2 + y_1^2. \tag{17}$$

One way to predetermine the distribution of the output energy of the butterfly is its concentration into one output element (energy compression)

$$y_0 = \sqrt{x_0^2 + x_1^2}, \tag{18}$$

$$y_1 = 0. \tag{19}$$

From (18) (19) it can be observed that the energy is concentrated in one output node of each butterfly. The presented method concentrates the signal energy in low indexed coefficients in transform domain. Information about the shape of the spectra is contained in the retained transformed space. When taking (13), (14) with the positive sign then according to (18) for the output of a butterfly one can write

$$ax_0 + bx_1 = \sqrt{x_0^2 + x_1^2}, \tag{20}$$

$$bx_0 - ax_1 = 0. \tag{21}$$

Addition of squares of Eq. (20), (21) yields

$$a^2 + b^2 = 1. \tag{22}$$

Then according to (20), (21)

$$a = \frac{x_0}{\sqrt{x_0^2 + x_1^2}}; \qquad b = \frac{x_1}{\sqrt{x_0^2 + x_1^2}}, \tag{23}$$

and from (13), (14)

$$c = b; \qquad d = a. \tag{24}$$

From the point of view of maximum compression (23), (24) we can define optimal transform coefficients of one butterfly of the fast $AWHT$.

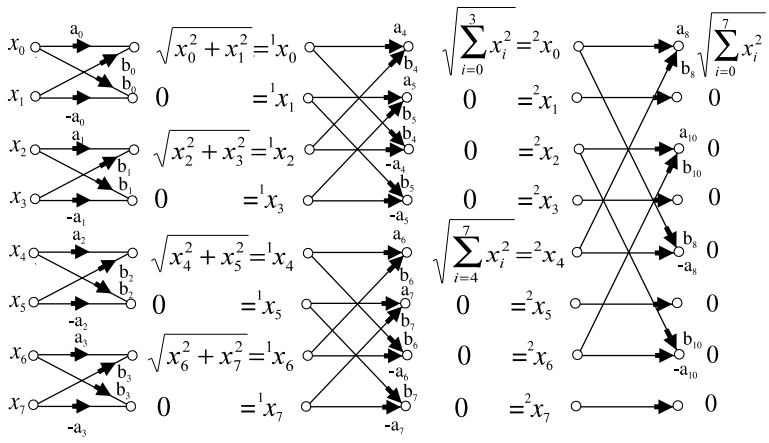

Fig. 6. Signal flow graph of the fast $AWHT^1$ for $N = 8$

Let us go ahead to a larger length. Let us take $N = 8$ and the degree $k = 1$ (Fig. 6) The butterfly coefficients in the iteration step 0 are

$$a_i = \frac{\sqrt{x_{2i}^2}}{\sqrt{x_{2i}^2 + x_{2i+1}^2}}; \qquad b_i = \frac{\sqrt{x_{2i+1}^2}}{\sqrt{x_{2i}^2 + x_{2i+1}^2}}, \tag{25}$$

where $i = 0, 1, 2, 3$. According to Fig. 6, ${}^1x_1 = {}^1x_3 = {}^1x_5 = {}^1x_7 = 0$ and thus using (23) in the iteration step 1 we cannot calculate the coefficients a_5, b_5, a_7, b_7. They can be set as desired. In each iteration step we divide the butterflies into groups. In the 0-th iteration step to 4 groups, in the first iteration step to 2 groups and finally in the second iteration step we leave one group. In practice it was proved that the repetition of leading coefficients for the whole group gives the best results. Then in our example in the first step we have

$$a_5 = a_4; \qquad b_5 = b_4; \tag{26}$$

and

$$a_7 = a_6; \qquad b_7 = b_6. \tag{27}$$

where the leading coefficients of each group are

$$a_4 = \frac{\sqrt{x_0^2 + x_1^2}}{\sqrt{x_0^2 + x_1^2 + x_2^2 + x_3^2}}; \qquad b_4 = \frac{\sqrt{x_2^2 + x_3^2}}{\sqrt{x_0^2 + x_1^2 + x_2^2 + x_3^2}}, \tag{28}$$

and

$$a_6 = \frac{\sqrt{x_4^2 + x_5^2}}{\sqrt{x_4^2 + x_5^2 + x_6^2 + x_7^2}}; \qquad b_6 = \frac{\sqrt{x_6^2 + x_7^2}}{\sqrt{x_4^2 + x_5^2 + x_6^2 + x_7^2}}. \tag{29}$$

In the following iteration step we stop the calculation (see algorithm (2)) in positions satisfying the condition $p \mod 2 \neq 0$, i.e. in the positions 1, 3, 5, 7. Analogously in the last iteration step the coefficients are

$$a_8 = a_{10} = \frac{\sqrt{x_0^2 + x_1^2 + x_2^2 + x_3^2}}{\sqrt{\sum_{i=0}^{7} x_i^2}}, \tag{30}$$

$$b_8 = b_{10} = \frac{\sqrt{x_4^2 + x_5^2 + x_6^2 + x_7^2}}{\sqrt{\sum_{i=0}^{7} x_i^2}}. \tag{31}$$

Generally for the transform coefficients of $AWHT^k$ in the leading positions of groups, one can write

$$a_{\frac{N\cdot s}{2}+2^s\cdot i} = \frac{\sqrt{\sum_{j=0}^{2^s-1} x_{2^{s+1}\cdot i+j}^2}}{\sqrt{\sum_{j=0}^{2^{s+1}-1} x_{2^{s+1}\cdot i+j}^2}}, \tag{32}$$

$$b_{\frac{N\cdot s}{2}+2^s\cdot i} = \frac{\sqrt{\sum_{j=0}^{2^s-1} x_{2^{s+1}\cdot i+2^s+j}^2}}{\sqrt{\sum_{j=0}^{2^{s+1}-1} x_{2^{s+1}\cdot i+j}^2}}, \tag{33}$$

where s denotes iteration step, $s \in \{1, \ldots, \log_2 N - 1\}, i$ denotes group number

$$i \in \{0, \ldots, \frac{N}{2^{s+1}} - 1\} \tag{34}$$

and N is the transform length. The other coefficients a, b in the positions where condition (2) is not satisfied are equal to the leading coefficients according to (32), (33), (34). The calculation is stopped in the positions where condition (2) is satisfied.

The inverse $AWHT$ of k-th degree can be calculated by applying the appropriate reverse ordered signal flow graph.

The computational complexity of $AWHT$ can be expressed by the number of additions (subtractions), which is the same as in the case of classical WHT,(4). Moreover the calculation of $AWHT$ of k-th degree requires

$$N_A = k \cdot N + 2(N - 2^k) \tag{35}$$

multiplications.

4 Adaptive compression method for multidimensional data

The basic compression scheme using adaptive Walsh-Haar transform is as follows

1. Determination of the reference vectors and adaptive transform matrices of appropriate degree.
2. Transformation of the signal using the calculated transform matrices.
3. Retention of the part of transformed signal (according to compression ratio given by eqs. (40), (41))
4. Reconstruction of the original signal using the inverse transform.

In calculation of adaptive transform matrices of $AWHT^k$ one has to apply the algorithms derived in the preceding sections. The question is how to create the transform matrices for multidimensional signals. Let us consider 2-dimensional signal $x(i,j)$, where $i,j \in \{0,\ldots,N-1\}$. We assume the same signal matrix length in both dimensions. Different transform matrices for each dimension will be constructed. In the matrix notation the transform of the signal $\mathbf{x}$ is [1]

$$\mathbf{y} = \mathbf{T}_1 \cdot \mathbf{x} \cdot \mathbf{T}_2^T, \tag{36}$$

where $\mathbf{T}_1$, $\mathbf{T}_2$ are $AWHT$ matrices. Then (36) can be expressed as

$$y(i,j) = \sum_{k=0}^{N-1} \sum_{l=0}^{N-1} T_1(i,k) \cdot T_2(j,l) \cdot x(k,l). \tag{37}$$

In general, the relation (36) for M-dimensional signal is

$$\begin{aligned} &y(i_1, i_2, \ldots, i_M) \\ &= \sum_{j_1=0}^{N-1} \sum_{j_2=0}^{N-1} \cdots \sum_{j_M=0}^{N-1} T_1(i_1,j_1) \cdot T_2(i_2,j_2) \cdot \ldots \cdot T_M(i_M,j_M) \cdot x(j_1,j_2,\ldots,j_M), \end{aligned} \tag{38}$$

where $i_1, i_2, \ldots, i_M \in \{0,1,\ldots,N-1\}$. The transform matrices $\mathbf{T}_1, \mathbf{T}_2, \ldots, \mathbf{T}_M$ $\left(AFWT^k, ACWT^k\right)$ can be set up in different ways. We have chosen the following procedure:

- for each dimension in M-dimensional spectrum we calculate integral-marginal 1 dimensional spectra, which represent reference vectors

$$\begin{aligned} S_1(i_1) &= \sum_{i_2=0}^{N_2-1} \sum_{i_3=0}^{N_3-1} \cdots \sum_{i_M=0}^{N_M-1} x(i_1, i_2, \cdots, i_M) \\ S_2(i_2) &= \sum_{i_1=0}^{N_1-1} \sum_{i_3=0}^{N_3-1} \cdots \sum_{i_M=0}^{N_M-1} x(i_1, i_2, \cdots, i_M) \\ &\vdots \\ S_M(i_M) &= \sum_{i_1=0}^{N_1-1} \sum_{i_2=0}^{N_2-1} \cdots \sum_{i_{M-1}=0}^{N_{M-1}-1} x(i_1, i_2, \cdots, i_M), \end{aligned} \tag{39}$$

where $i \in \{0, 1, \ldots, N-1\}$.

- using reference vectors S_l we calculate the coefficients of the transform matrix $\mathbf{T}_l$ according to the algorithm derived in the section 3; $l \in \{1, 2, \ldots, M\}$.

The reference vectors are determined from the signal $\mathbf{x}$ that is to be compressed. For each signal $\mathbf{x}$ new reference vectors and thus transform matrices must be determined. Information about the shape of the signal is contained in the retained coefficients in the transform domain and in the transform matrices derived from reference vectors.

The presented method concentrates the signal energy in low spaced coefficients in the transform domain so that we can use zonal filtration [6]. The transformed area $i_1, i_2, \ldots, i_M \in \{0, \ldots, N-1\}$ is divided into two subregions. The coefficients are retained in the subregion

$$\begin{aligned} i_1 &\in \{0, 1, \ldots, k_1 - 1\} \\ i_2 &\in \{0, 1, \ldots, k_2 - 1\} \\ &\vdots \\ i_M &\in \{0, 1, \ldots, k_M - 1\}, \end{aligned} \tag{40}$$

where $k_1, k_2, \ldots, k_M \leq N$. When carrying out the direct transformation according to (38) it is sufficient to calculate only the coefficients belonging to this subregion. Other coefficients entering the inverse transform can be replaced either by the mean value or by zero. The compression ratio is then

$$CR = \frac{N^M}{k_1 \cdot k_2 \cdot \ldots \cdot k_M}. \tag{41}$$

The compression ratio is decreased by the necessity to store the reference vectors S_1, S_2, …, S_M. When we realize that the length of each reference vector is approximately hundreds or thousands elements, we can see that their storage decreases the compression ratio (41) only a little.

5 Results

Experimental progress in the understanding of nuclear structure depends critically on the ability to analyse coincidence data in multidimensional space. The method proposed in the paper considerably decreases the memory needed to store multidimensional signals, which are in our case nuclear histograms (spectra). To compare the efficiency and quality of the above mentioned transforms we have chosen several examples of nuclear spectra. In Fig. 7a we present 2-dimensional 256x256 channels spectrum - SPECTRUM 1 - acquired in coincidence measurement of the Doppler broadening of the annihilation line and positron lifetime [7], [8]. We have transformed the spectrum using WHT^7, $AWHT^7$ and Cosine transforms. From the point of view of compression the Cosine transform is considered to be suboptimal [9]. The efficient algorithms to calculate Cosine transforms are presented in [10], [11]. According to the compression method described in the previous section after each transformation we have retained only low-indexed coefficients (zonal filtration with $CR = 64$) and then using appropriate inverse

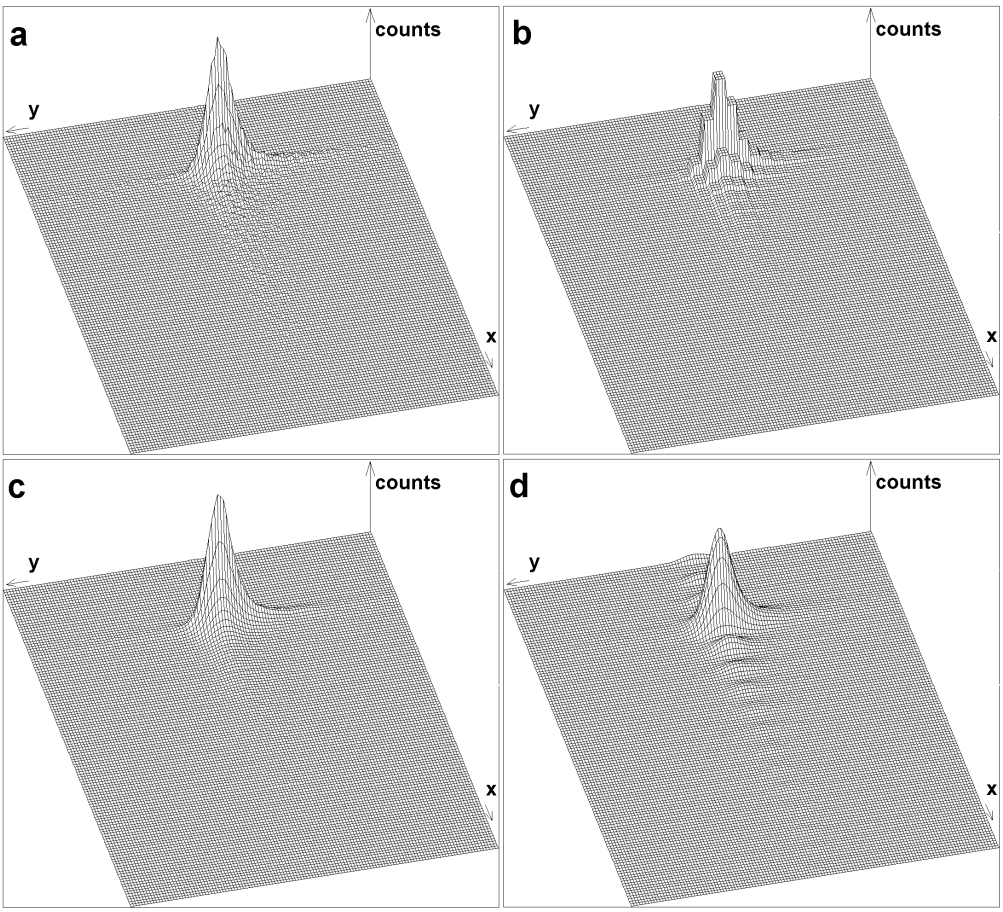

Fig. 7. Original (a) and reconstructed 2-dimensional nuclear spectra ($CR = 64$) using WHT^7 (b), $AWHT^7$ (c) and Cosine transform (d)

transform we have transformed these data back. The results are shown in Figs. 7b, c, d. One can see that by using WHT^7 (Fig. 7b) the artificial square structure appears in the spectrum. On the other hand when employing $AWHT^7$ good fidelity with the original spectrum can be observed (Fig. 7c). This spectrum is smoother than the original spectrum. This can be a desirable effect. Employing Cosine transforms gives a smooth result, however, the spectrum contains unnatural oscillations (Fig. 7d).

In the next experiment using the same compression ratio ($CR = 64$) we have studied the influence of transform degree to quality of compression for $WHT^{5,2,1,0}$ (Figs. 8a, b, c, d). We can observe that up to degree 2 the result is practically the same as for degree 7 (Fig. 7b). However for degrees 1, 0 the shape of the spectrum is completely destroyed.

We have carried out the same experiment but this time employing $AWHT^{5,2,1,0}$ (Figs. 9a, b, c, d). For all transform degrees the results are in very good agreement with the origi-

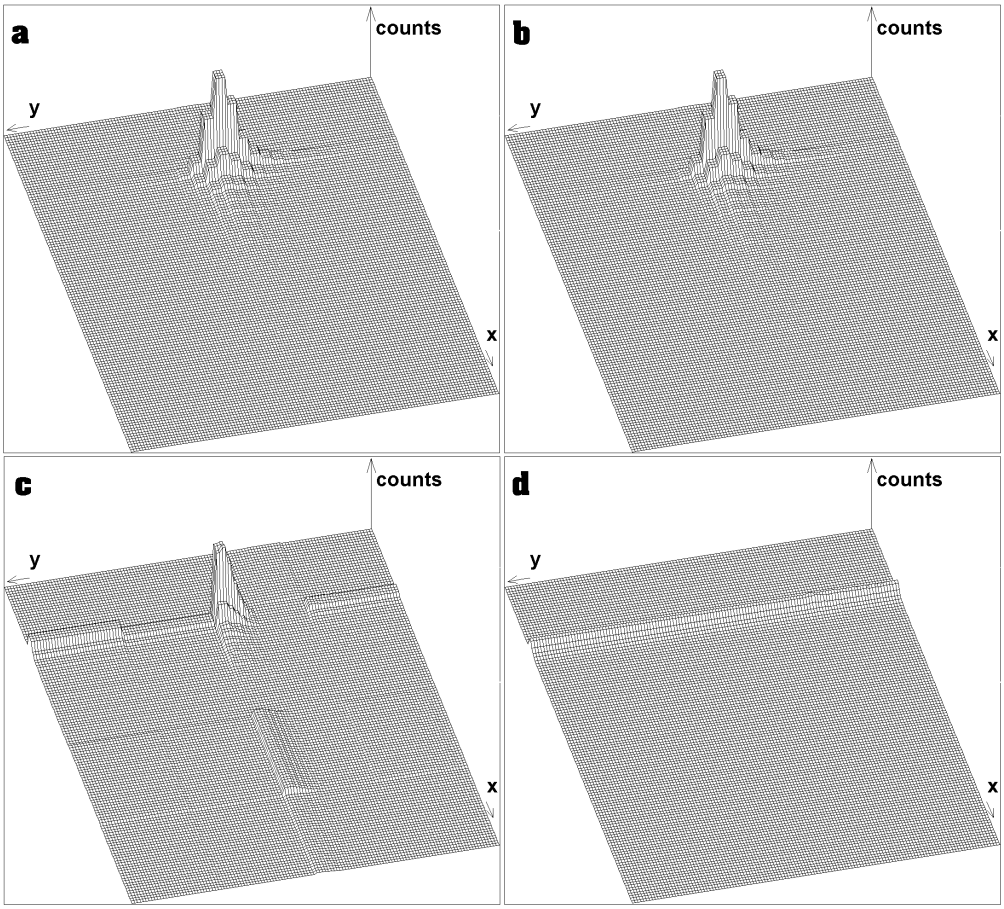

Fig. 8. Reconstructed 2-dimensional nuclear spectra (from Fig. 7a with $CR = 64$) using WHT^5 (a), WHT^2 (b), WHT^1 (c) and WHT^0 (d)

nal spectrum.

In the next example we have taken spectrum of γ-radiation accompanying the fission of ^{252}Cf - SPECTRUM 2. The large amount of data (4096 channels in each dimension) has been collected using multidetector system (20 detectors). Again the aim was to decrease the data volume without a loss of important information. In this case we have spectrum with narrow peaks and more complicated background (Fig. 10a). We have chosen compression ratio $CR = 32$. The results using WHT^7, $AWHT^7$ and Cosine transform are shown in Figs. 10b, c, d, respectively. From visual comparison apparently the $AWHT^7$ preserves the shape of the spectrum with the best quality.

The influence of transform degree on the spectrum form for $WHT^{5,2,1,0}$ is shown in Figs. 11a, b, c, d and for $AWHT^{5,2,1,0}$ in Figs. 12a, b, c, d, respectively. One can see that by decreasing the degree the two dominant peaks in the spectrum are becoming narrower and higher and approach

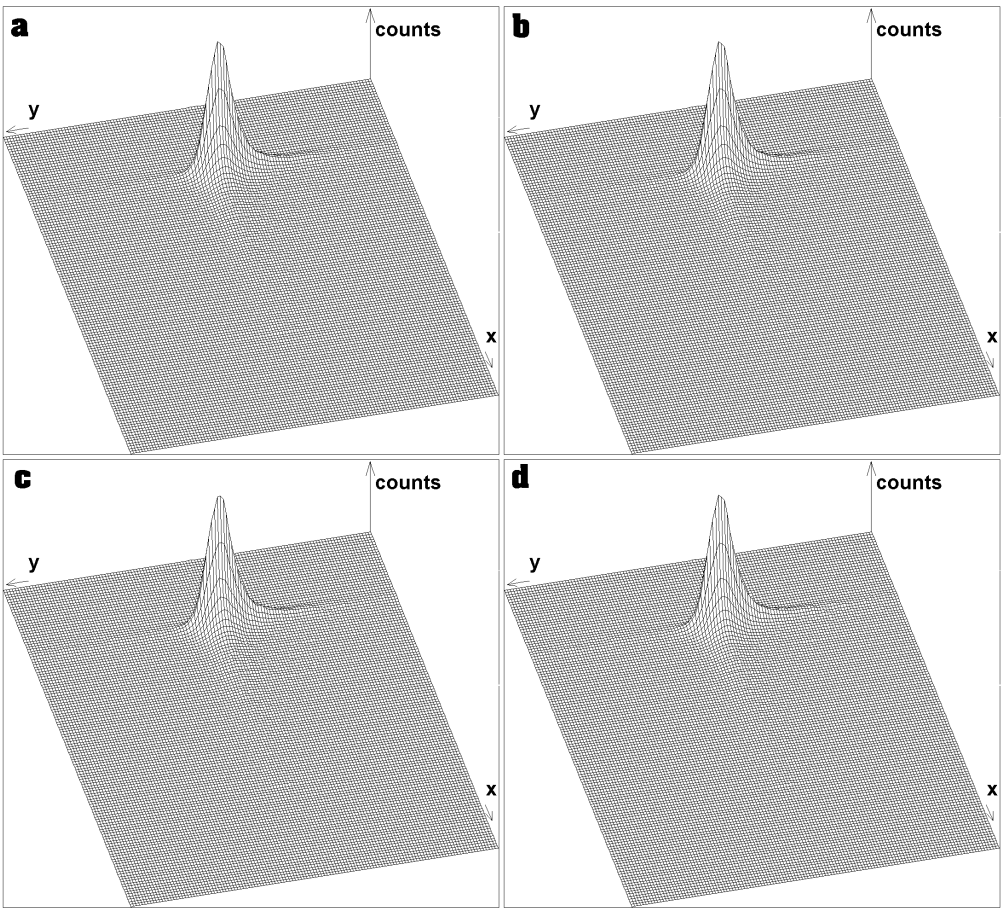

Fig. 9. Reconstructed 2-dimensional nuclear spectra (from Fig. 7a with $CR = 64$) using $AWHT^5$ (a), $AWHT^2$ (b), $AWHT^1$ (c) and $AWHT^0$ (d)

to the peak form in the original spectrum (Fig. 10a).

In the third example we have taken 2-dimensional slice from the data cube of 3-fold $\gamma-\gamma-\gamma$ coincidences [12] shown in Fig. 13a - SPECTRUM 3. We have repeated the same experiment as in the previous two examples ($CR = 64$). Hence Figs. 13b, c, d show the spectrum compressed via WHT^7, $AWHT^7$ and Cosine transform, respectively. The experiences from two above presented examples have been confirmed. $AWHT^7$ is the best of all three transforms.

Fig. 14 illustrates the influence of transform degree of $WHT^{5,2,1,0}$ to the form of compressed spectrum. It can be seen that for degrees 1, 0 (Figs. 14c, d) the original spectral information is completely lost. As to adaptive transforms we can observe that $AWHT^{5,2}$ (Figs. 15a, b) essentially preserve the original spectrum. $AWHT^{1,0}$ (Figs. 15c, d) generate new non-existing peaks. Efficiency of the transform depends on the type of processed data. While in Fig. 12, which contains narrow peaks, the best results were obtained using $AWHT^0$, in Fig. 15 (spectrum with

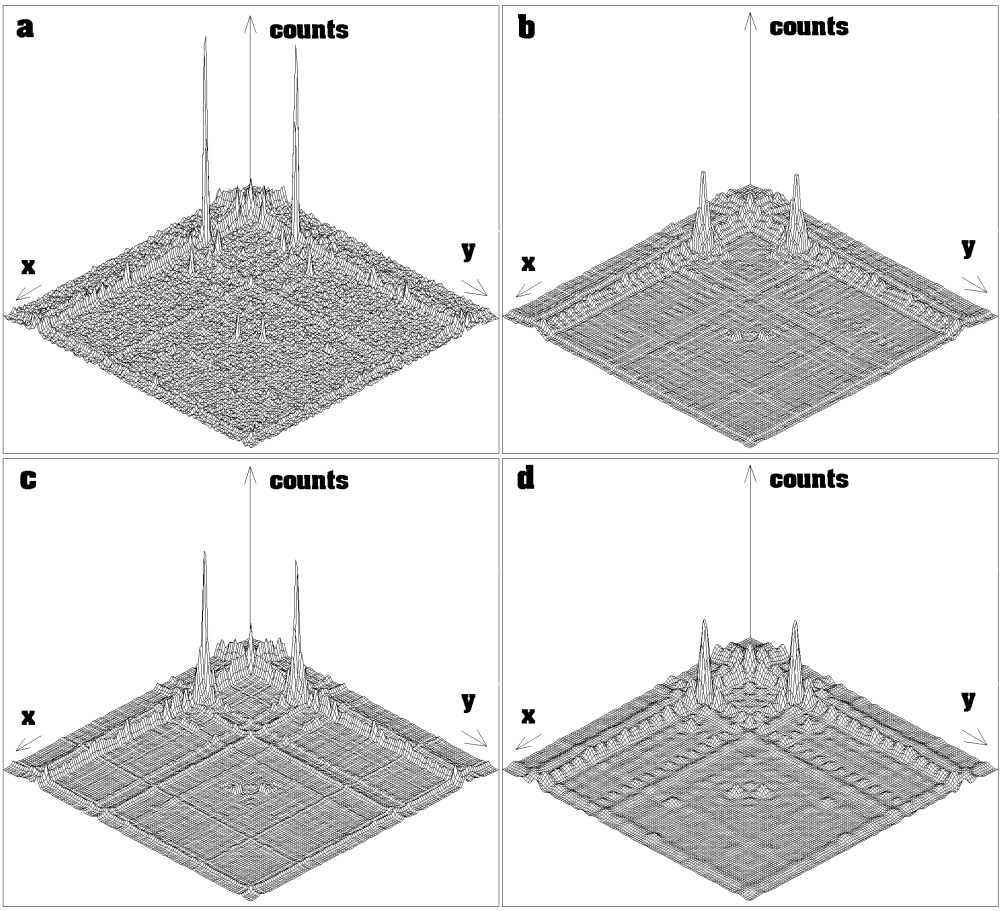

Fig. 10. Original (a) and reconstructed 2-dimensional nuclear spectra ($CR = 32$) using WHT^7 (b), $AWHT^7$ (c) and Cosine transform (d)

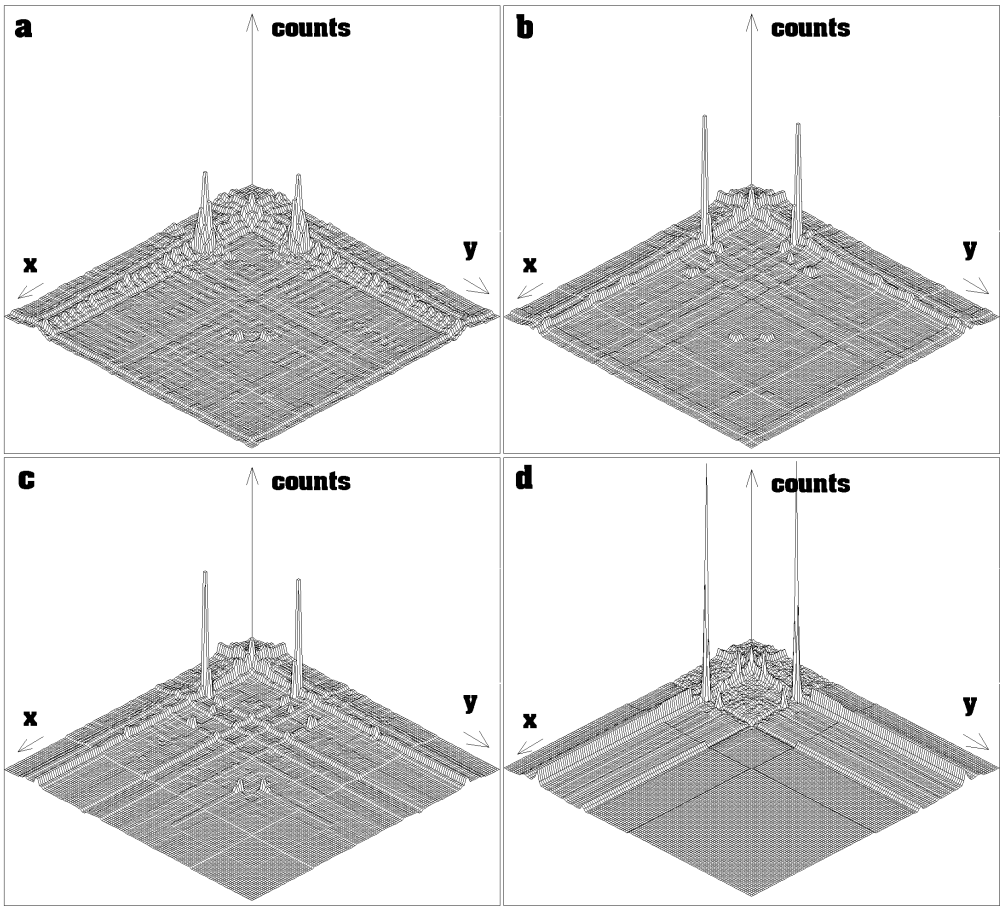

Fig. 11. Reconstructed 2-dimensional nuclear spectra (from Fig. 10a with $CR = 32$) using WHT^5 (a), WHT^2 (b), WHT^1 (c) and WHT^0 (d)

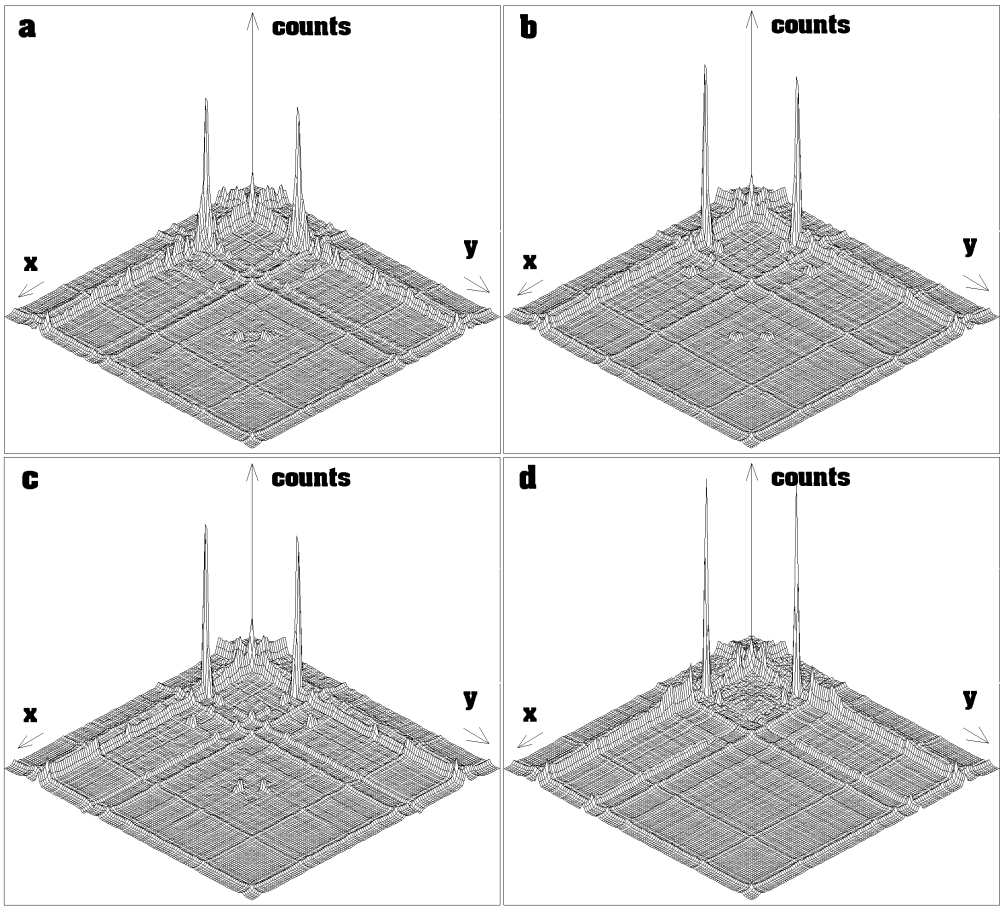

Fig. 12. Reconstructed 2-dimensional nuclear spectra (from Fig. 10a with $CR = 32$) using $AWHT^5$ (a), $AWHT^2$ (b), $AWHT^1$ (c) and $AWHT^0$ (d)

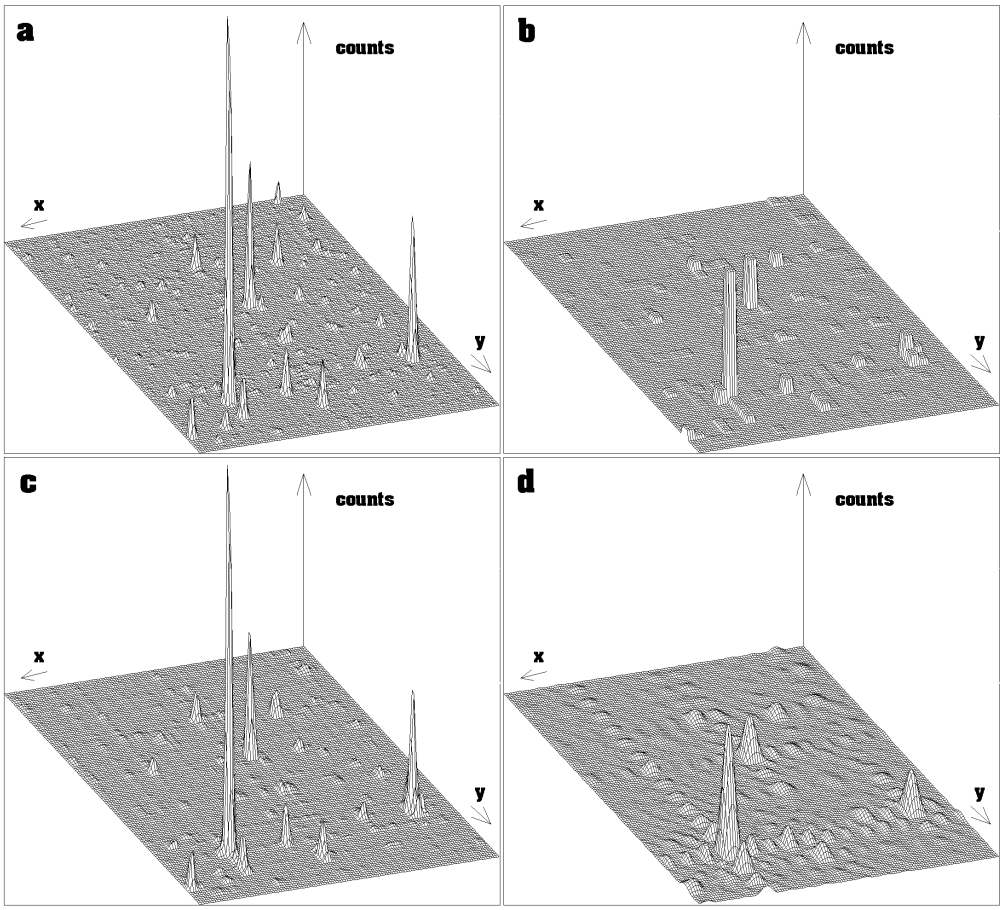

Fig. 13 Original (a) and reconstructed 2-dimensional nuclear spectra ($CR = 64$) using WHT^7 (b), $AWHT^7$ (c) and Cosine transform (d)

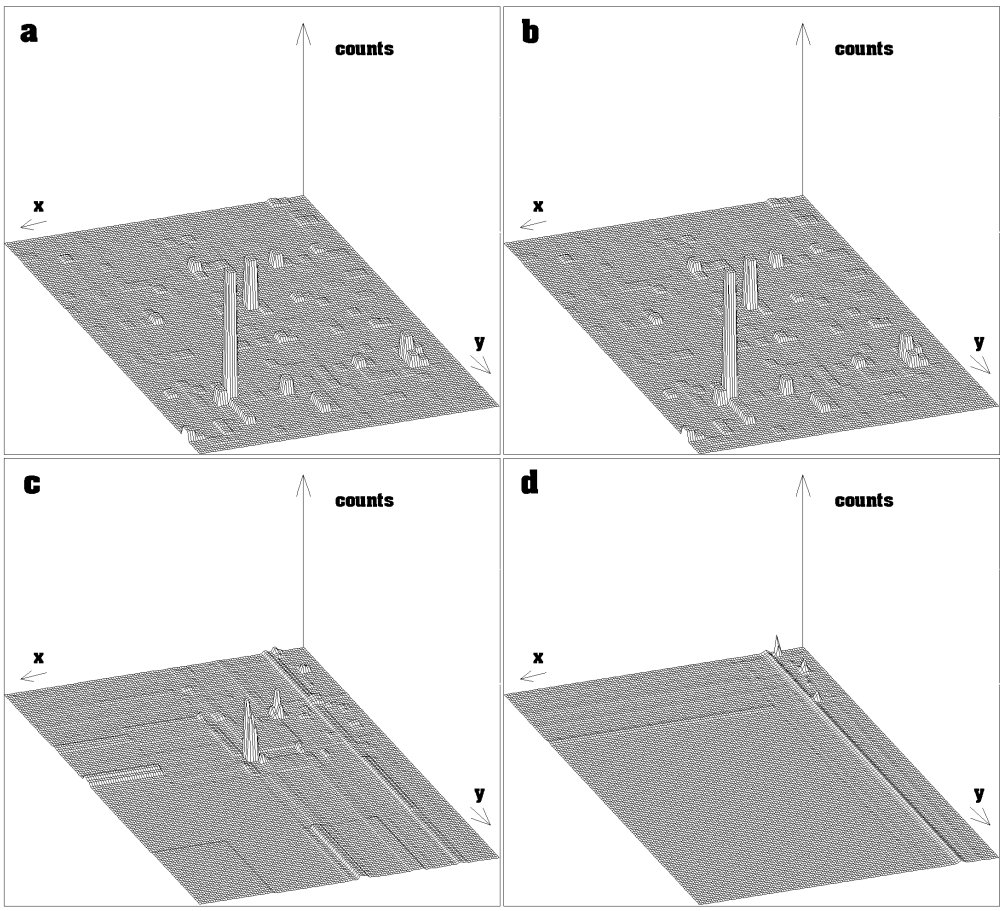

Fig. 14. Reconstructed 2-dimensional nuclear spectra (from Fig. 5a with $CR = 64$) using WHT^5 (a), WHT^2 (b), WHT^1 (c) and WHT^0 (d)

wider peaks), the best results were obtained by using $AWHT^2$.

In [13] a function of energy packing efficiency is introduced. It is defined as a part of energy contained in the first M from N transformed coefficients

$$EPE(M) = \frac{\sum_{i=0}^{M-1} y_i^2}{\sum_{i=0}^{N-1} y_i^2} \cdot 100[\%]. \tag{42}$$

In the transform domain of multidimensional orthogonal transforms described so far the energy is concentrated around the null point of the coordinate system. Therefore analogously to

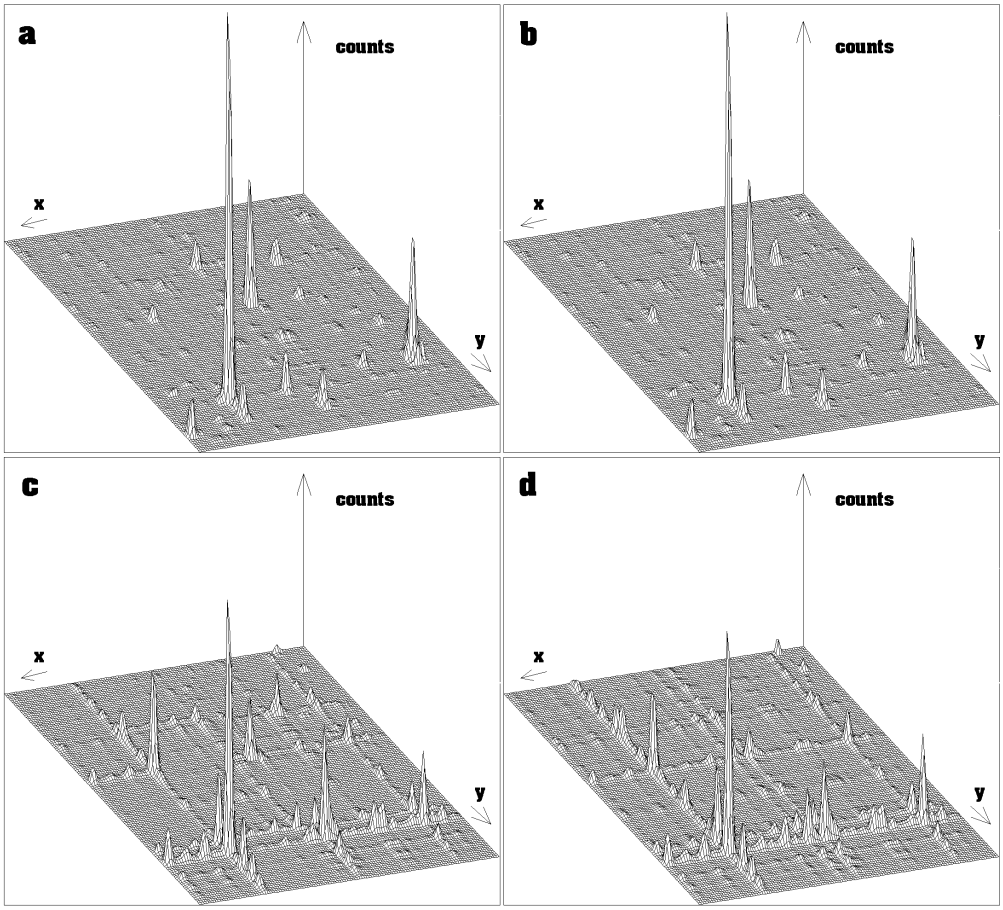

Fig. 15. Reconstructed 2-dimensional nuclear spectra (from Fig. 13a with $CR = 64$) using $AWHT^5$ (a), $AWHT^2$ (b), $AWHT^1$ (c) and $AWHT^0$ (d)

(42) we introduce the energy packing efficiency function for the 2-dimensional transform

$$EPE(M) = \frac{\sum_{i=0}^{M-1} \sum_{j=0}^{M-1} y_{i,j}^2}{\sum_{i=0}^{N-1} \sum_{j=0}^{N-1} y_{i,j}^2} \cdot 100[\%]. \tag{43}$$

Further let us define the average value of $EPE(M)$ function

$$AEPE = \frac{\sum_{i=0}^{N-1} EPE(i)}{N}. \tag{44}$$

This coefficient corresponds in a way to overall compression efficiency of a transform.

Fig. 16 presents EPE(M) functions and AEPE coefficients for WHT^{0-7} and for SPECTRUM 1 (Fig. 7a). From Fig. 16 it follows that WHT^3 is the most efficient transform for this type of spectrum.

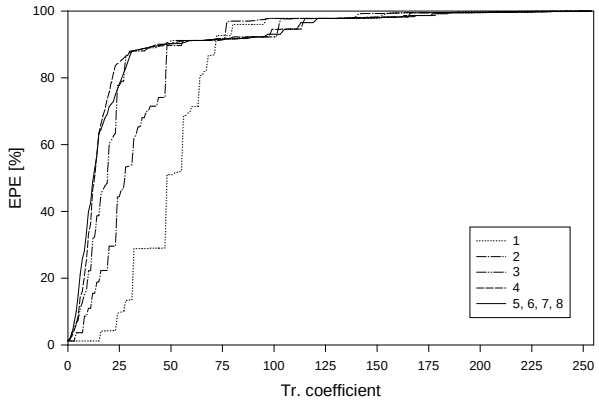

Fig. 16. EPE functions for the spectrum from Fig. 7a and the following transforms: 1-WHT^0 ($AEPE = 79.66$), 2-WHT^1 ($AEPE = 86.69$), 3-WHT^2 ($AEPE = 89.78$), 4-WHT^3 ($AEPE = 90.83$), 5-WHT^4 ($AEPE = 90.71$), 6-WHT^5 ($AEPE = 90.67$), 7-WHT^6 ($AEPE = 90.64$), 8-WHT^7 ($AEPE = 90.64$)

The EPE functions and $AEPE$ coefficients for the same spectrum and different degrees of $AWHT$ is shown in Fig. 17. In this case for all degrees the compression efficiency is very high.

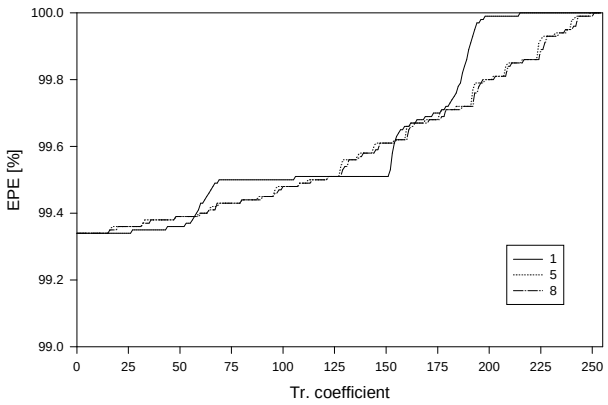

Fig. 17. EPE functions for the spectrum from Fig. 7a and the following transforms: 1-$AWHT^0$ ($AEPE = 99.62$), 5-$AWHT^4$ ($AEPE = 99.59$), 8-$AWHT^7$ ($AEPE = 99.59$)

In the same manner we have estimated the compression efficiency for SPECTRUM 2 (Fig. 10a) for WHT^{0-7} (Fig. 18) and $AWHT^{0-7}$ (Fig. 19). In both cases the dependencies EPE for the degrees 3,4,5,6,7 are practically identical. Also the $AEPE$ coefficients change very slightly. On the other hand the differences between classical and adaptive transforms are observable.

Finally the EPE dependencies and $AEPE$ coefficients are shown for WHT^{0-7} in Fig. 20 and for $AWHT^{0-7}$ in Fig. 21, respectively. Again the EPE functions and AEPE coefficients for WHT^{4-7} and $AWHT^{4-7}$ are practically identical. However the difference of the compression efficiency between classical and adaptive transforms is in this case substantial.

At last we have compared the efficiency of WHT^7 (Walsh transform), WHT^0 (Haar transform), $AWHT^7$ and Cosine transform for SPECTRUM 1, 2, 3 (Figs. 22, 23, 24). One can conclude that in all three cases $AWHT^7$ compresses two dimensional spectra in the most efficient way.

For illustration purposes we introduce also the example of a part of three dimensional spectrum (256x256x256 channels) [14], [15]. The sizes of balls representing channels are proportional to channel contents. Fig. 25 presents the original spectrum and Fig. 26 presents the same spectrum after the compression via $AWHT^7$ and $CR = 32$. The sizes of balls are proportional to the channel counts. We can observe that basic features of the spectrum after the compression remain retained. In Fig. 27 we present the picture of a two dimensional nuclear spectrum obtained directly from experimental data (Fig. 25) where all channels along one dimension were integrated. The same nuclear spectrum decompressed from our compressed nuclear spectrum from Fig. 26 is given in Fig. 28. The next couple of spectra, now obtained by integration along another dimension, are shown in Figs. 29, 30. The good fidelity of two dimensional decompressed spectra (Figs. 28 and 30)can be observed.

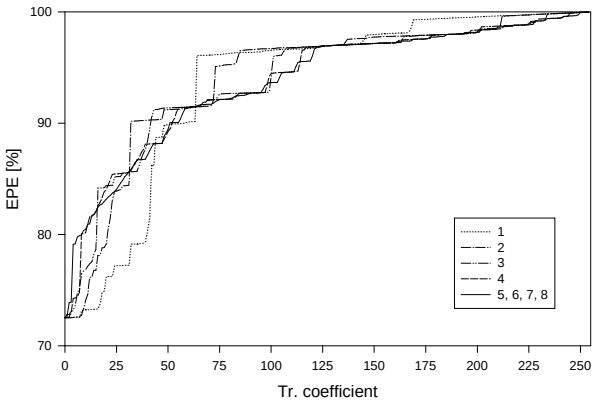

Fig. 18. EPE functions for the spectrum from Fig. 10a and the following transforms: 1-WHT^0 ($AEPE = 93.73$), 2-WHT^1 ($AEPE = 94.27$), 3-WHT^2 ($AEPE = 93.97$), 4-WHT^3 ($AEPE = 93.83$), 5-WHT^4 ($AEPE = 93.77$), 6-WHT^5 ($AEPE = 93.72$), 7-WHT^6 ($AEPE = 93.71$), 8-WHT^7 ($AEPE = 93.71$)

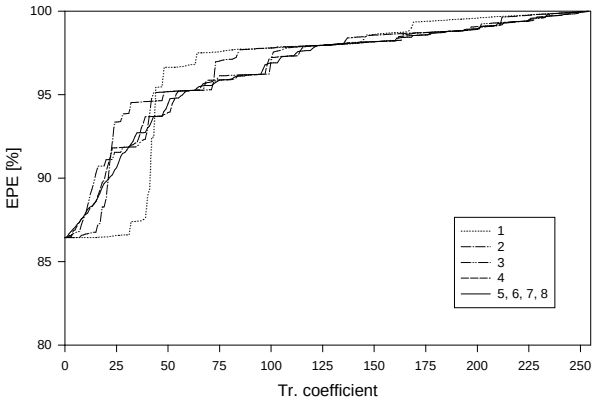

Fig. 19. EPE functions for the spectrum from Fig. 10a and the following transforms: 1-$AWHT^0$ ($AEPE = 96.52$), 2-$AWHT^1$ ($AEPE = 96.86$), 3-$AWHT^2$ ($AEPE = 96.64$), 4-$AWHT^3$ ($AEPE = 96.54$), 5-$AWHT^4$ ($AEPE = 96.48$), 6-$AWHT^5$ ($AEPE = 96.44$), 7-$AWHT^6$ ($AEPE = 96.42$), 8-$AWHT^7$ ($AEPE = 96.42$)

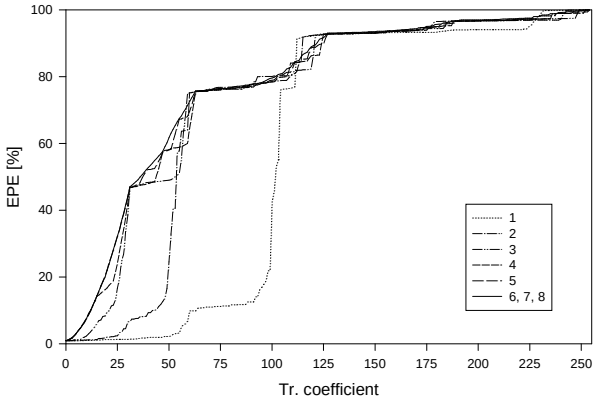

Fig. 20. EPE functions for the spectrum from Fig. 13a and the following transforms: 1-WHT^0 ($AEPE = 58.78$), 2-WHT^1 ($AEPE = 72.37$), 3-WHT^2 ($AEPE = 75.83$), 4-WHT^3 ($AEPE = 76.78$), 5-WHT^4 ($AEPE = 77.57$), 6-WHT^5 ($AEPE = 77.85$), 7-WHT^6 ($AEPE = 77.9$), 8-WHT^7 ($AEPE = 77.91$)

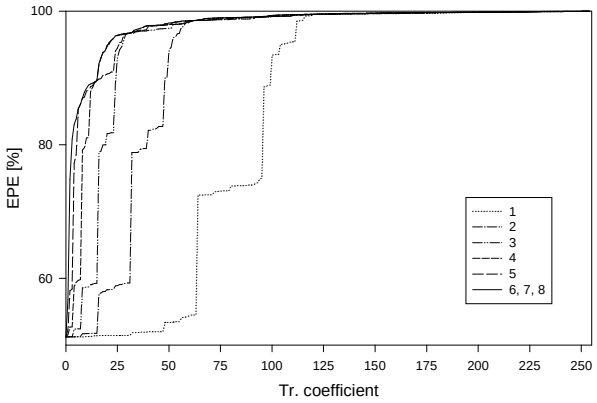

Fig. 21. EPE functions for the spectrum from Fig. 13a and the following transforms: 1-$AWHT^0$ ($AEPE = 84.13$), 2-$AWHT^1$ ($AEPE = 92.63$), 3-$AWHT^2$ ($AEPE = 95.83$), 4-$AWHT^3$ ($AEPE = 97.15$), 5-$AWHT^4$ ($AEPE = 97.84$), 6-$AWHT^5$ ($AEPE = 98.08$), 7-$AWHT^6$ ($AEPE = 98.11$), 8-$AWHT^7$ ($AEPE = 98.11$)

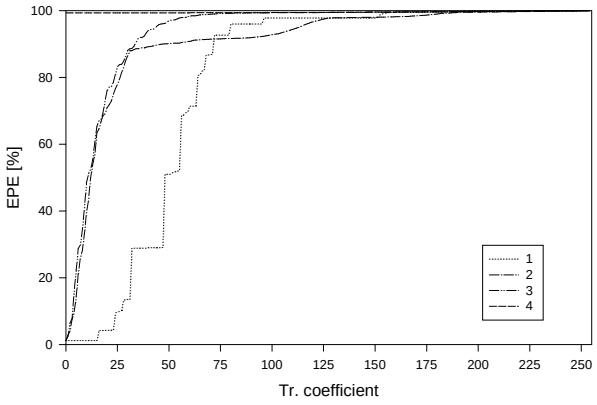

Fig. 22. EPE functions for the spectrum from Fig. 7a and the following transforms: 1 - Haar transform, 2 - WHT^7, 3 - Cosine transform, 4 - $AWHT^7$

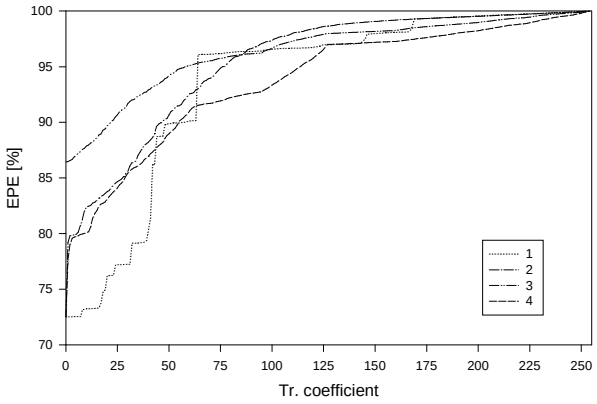

Fig. 23. EPE functions for the spectrum from Fig. 10a and the following transforms: 1 - Haar transform, 2 - Cosine transform, 3 - $AWHT^7$, 4 - WHT^7

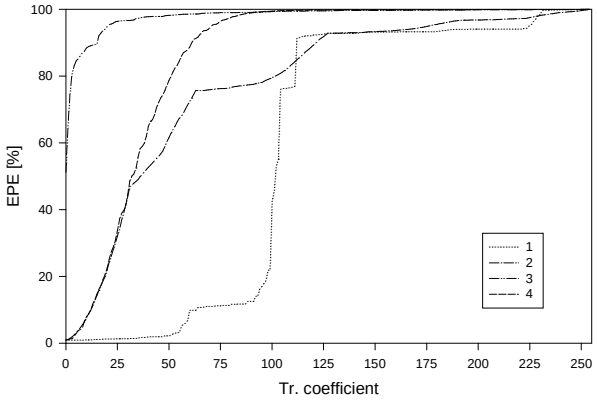

Fig. 24. EPE functions for the spectrum from Fig. 13a and the following transforms: 1 - Haar transform, 2 - WHT^7, 3 - $AWHT^7$, 4 - Cosine transform

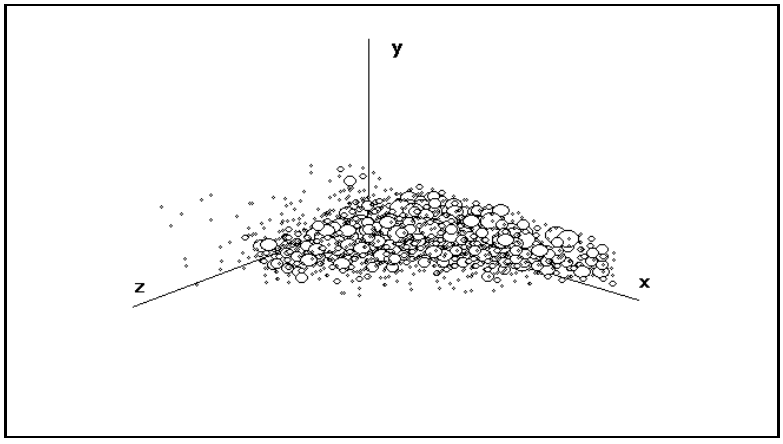

Fig. 25. Three-dimensional original nuclear spectrum

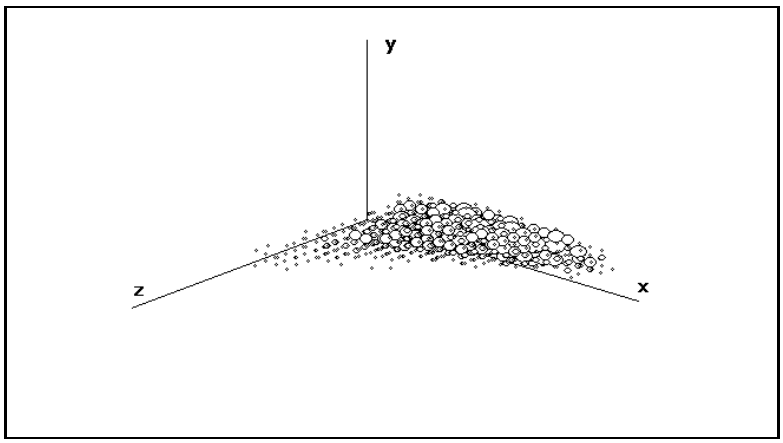

Fig. 26. Three-dimensional reconstructed spectrum after the compression using $AWHT^7$ and $CR = 32$

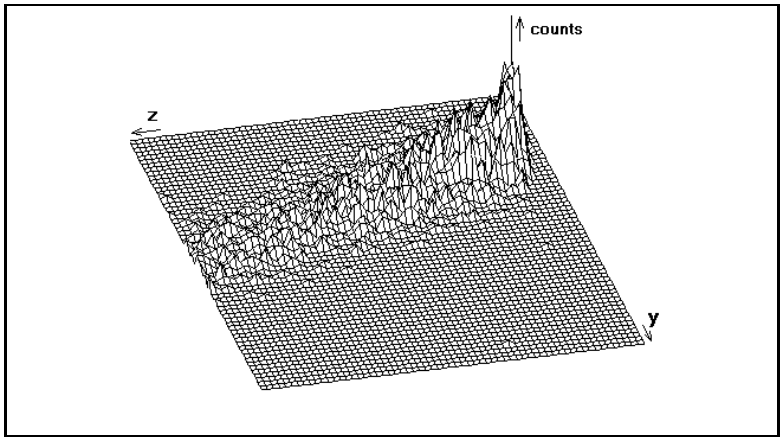

Fig. 27. Example of two dimensional original nuclear spectrum (from Fig. 25) - projection of the x axis on the y, z plane.

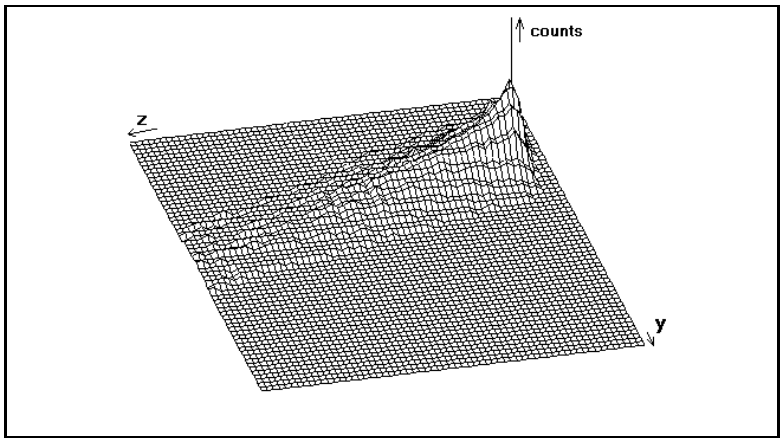

Fig. 28. Example of two dimensional decompressed nuclear spectrum from Fig. 26 - projection of the x axis on the y, z plane.

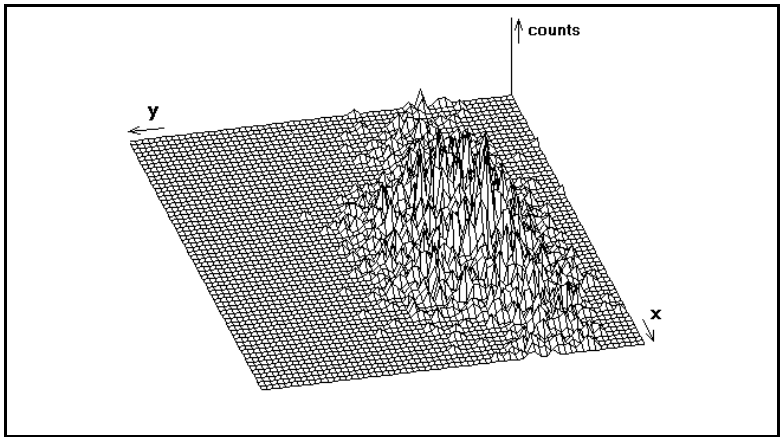

Fig. 29. Example of two dimensional original nuclear spectrum (from Fig. 25) - projection of the z axis on the x, y plane.

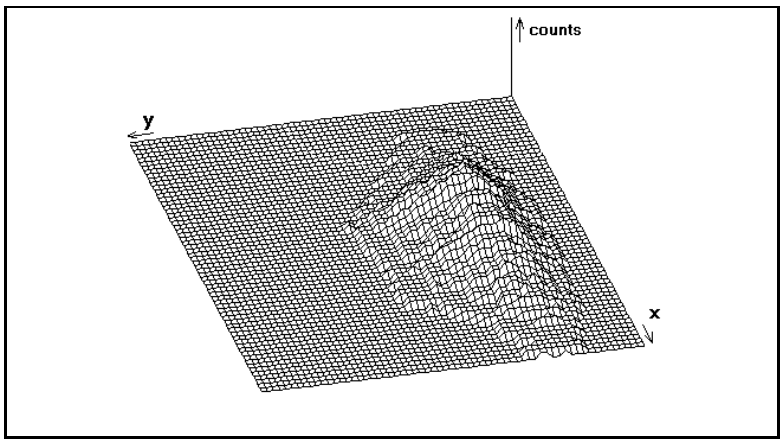

Fig. 30. Example of two dimensional decompressed nuclear spectrum from Fig. 26 - projection of the z axis on the x, y plane.

6 Conclusions

In the paper we have defined a sequence of new adaptive transforms. The necessary and sufficient conditions assuring the orthonormality of AWHT are given by eqs. (9), (10), (11), (13), (14) The goal is to achieve maximum possible compression of the multidimensional block data with acceptable signal distortion. The algorithms were tested for several 2-dimensional and also 3-dimensional nuclear spectra. In addition to visual comparison also the compression efficiencies have been evaluated. In all examples presented the results achieved through the use of adaptive transforms were better than those of classical transforms.

Besides of this, for both classical and adaptive transforms, the influence of transform degree on the quality and efficiency of the compression has been studied as well. It was observed that from the point of view of compression efficiency it is not necessary to employ the highest possible transform degree ($k = \log_2 N - 1$). In some cases the increasing transform degree deteriorates the compression efficiency. Lower transform degree means less number of operations and thus the speed up of the transformation. The computational complexity of WHT is given by (4) and AWHT by (35).

References

[1] A. N., Rao K.R.: *Orthogonal Transforms for Digital Signal Processing*, Springer, Berlin 1975

[2] K.G. Beauchamp: *Walsh Functions and Their Applications*, Academic Press, London, New York, San Francisco 1975

[3] D.F. Elliot, K.R.Rao: *Fast Transforms, Algorithms, Analyses, Applications*, Academic Press, Orlando 1982

[4] L. Jaroslavskij, I. Bajla: *Methods and systems of digital image processing*, (In slovak). Alfa, Bratislava 1989

[5] K.R. Rao et al.: *IEEE Trans.* **ASSP-24** (1976)

[6] M. Morháč, V. Matoušek: *in Proc. Computer Analysis of Images and Patterns, International Fair Symposium, Leipzig, Germany 1989*. p. 28-29

[7] K. Krištiaková et al.: *in Proc. Slow Positron Beam Techniques for Solids and Surfaces, Jackson Hole, Wyoming, USA 1992*p. 150

[8] J. Krištiak, K. Krištiaková, O. Šauša, J. Bartoš: *Journal de Physique* **IV** (1993) 265

[9] K.R. Rao, P. Yip: *Discrete Cosine Transform*, Academic Press, Inc., Boston, San Diego, New York, London, Sydney, Tokyo, Toronto 1990

[10] V. Britaňák: *Signal processing* **40** (1994) 183-194

[11] V. Britaňák: *Applied signal processing* **1** (1994) 76-93

[12] J. Kliman et al.: *in 7-th Int. School of Neutron Physics, Ratmino 1995*, (ed. E. Kornilov), Lectures, Vol.2 1995, p. 483

[13] H. Kitajima: *IEEE Transactions on Commun.* **COM-24** (1976) 1256-1258

[14] S. Hlaváč et al.: *Final Report for the IAEA Research Contract* No. 6970/Rb 1994

[15] S. Hlaváč et al.:*in Conf. on Nuclear Data for Science and Technology, Gatlinburg, TN, USA* 1994